Quantum squeezing via self-induced transparency in a photonic crystal fiber

M. S. Najafabadi, [1] G. Leuchs [1,4]

[1] Max Planck Institute for the Science of Light, Erlangen, Germany

[4] Friedrich-Alexander-Universität Erlangen-Nürnberg, Erlangen, Germany

May 10, 2024
Kenya summer school

Soliton

John Scott Russell (1834): observation of a solitary wave in water on the Union Canal near Edinburgh

Collision of solitons in shallow water

Solitons development in optical fiber

year	**discovery**
1973	Akira Hasegawa of AT and T Bell Labs.
1987	Emplit et al. the Universities of Brussels and Limoges
1988	Linn F. Mollenauer , optical gain
...	...
2008	D. Y. Tang et al. higher-order vector soliton observation

Atom Field interaction

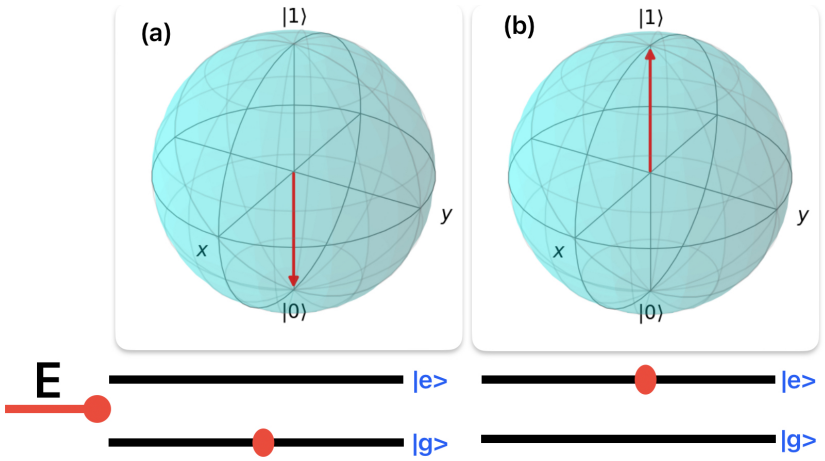

Pulse area

$$\mathbf{E(z,t)} = \mathcal{E}\exp(-\mathbf{i}\phi(\mathbf{ikz} - \omega\mathbf{t})) + \mathbf{c.c}$$

$$\mathbf{\Omega} = (\tfrac{\mathbf{2d}}{\hbar})\mathcal{E} \rightarrow \textbf{Rabi Frequency}$$

$$\text{Area} = \int_{-\infty}^{\mathbf{t}} \mathbf{\Omega(z,t')dt'}$$

π pulse

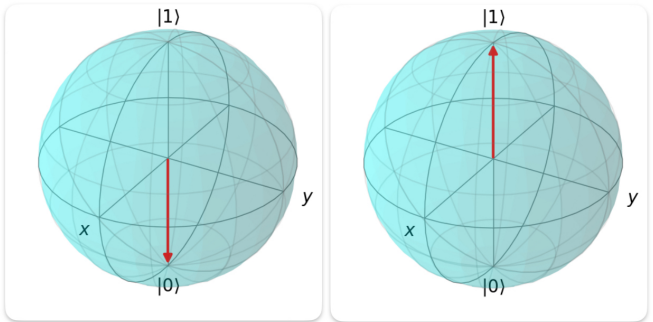

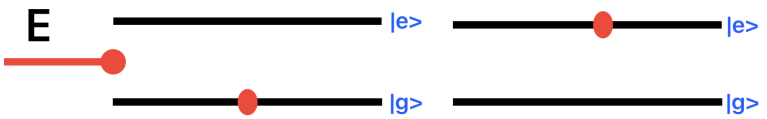

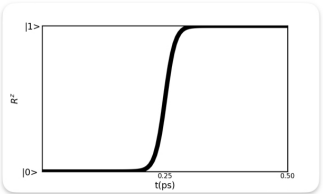

2π Pulse

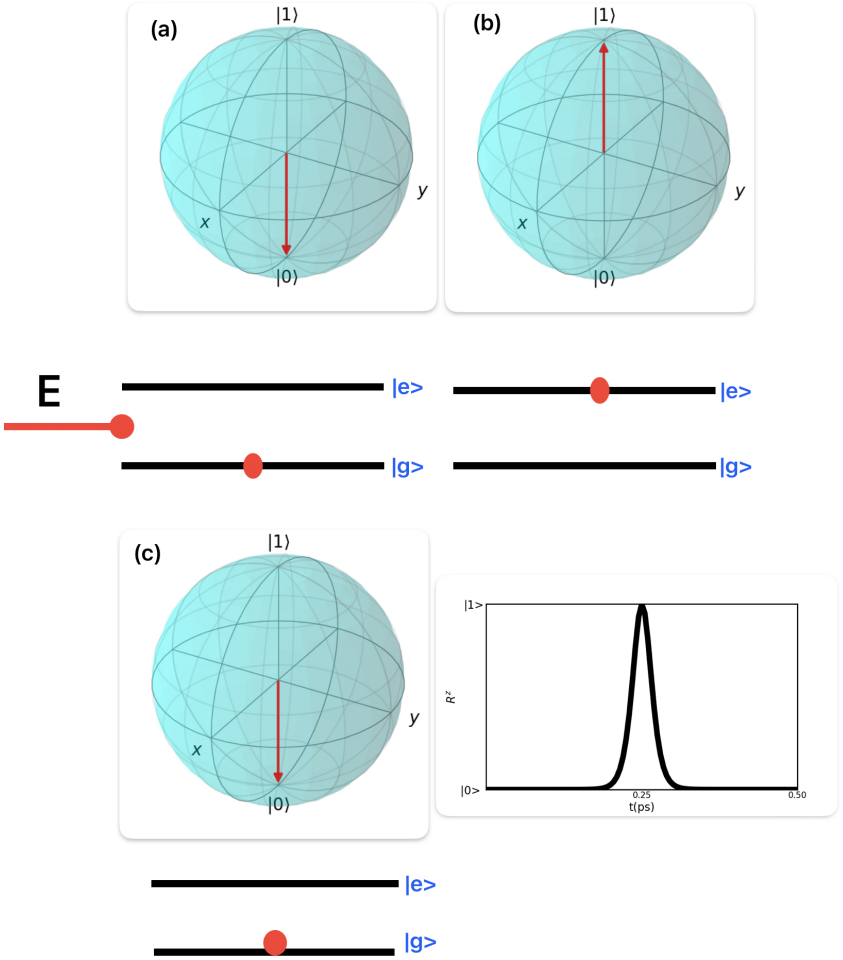

2π pulse

3π pulse

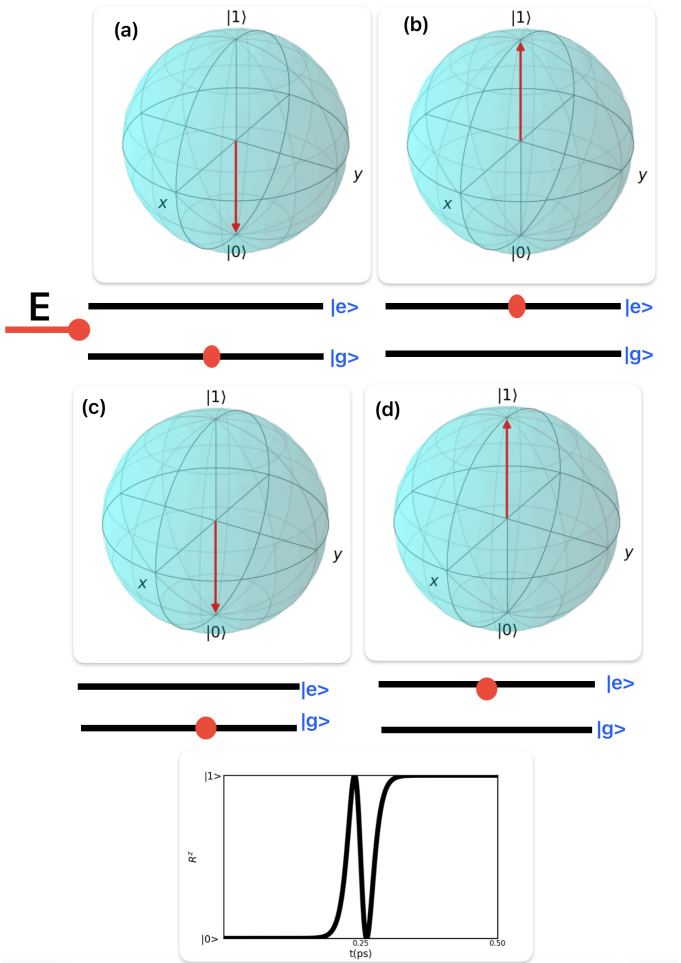

3π pulse

$\frac{\pi}{2}$ propagation

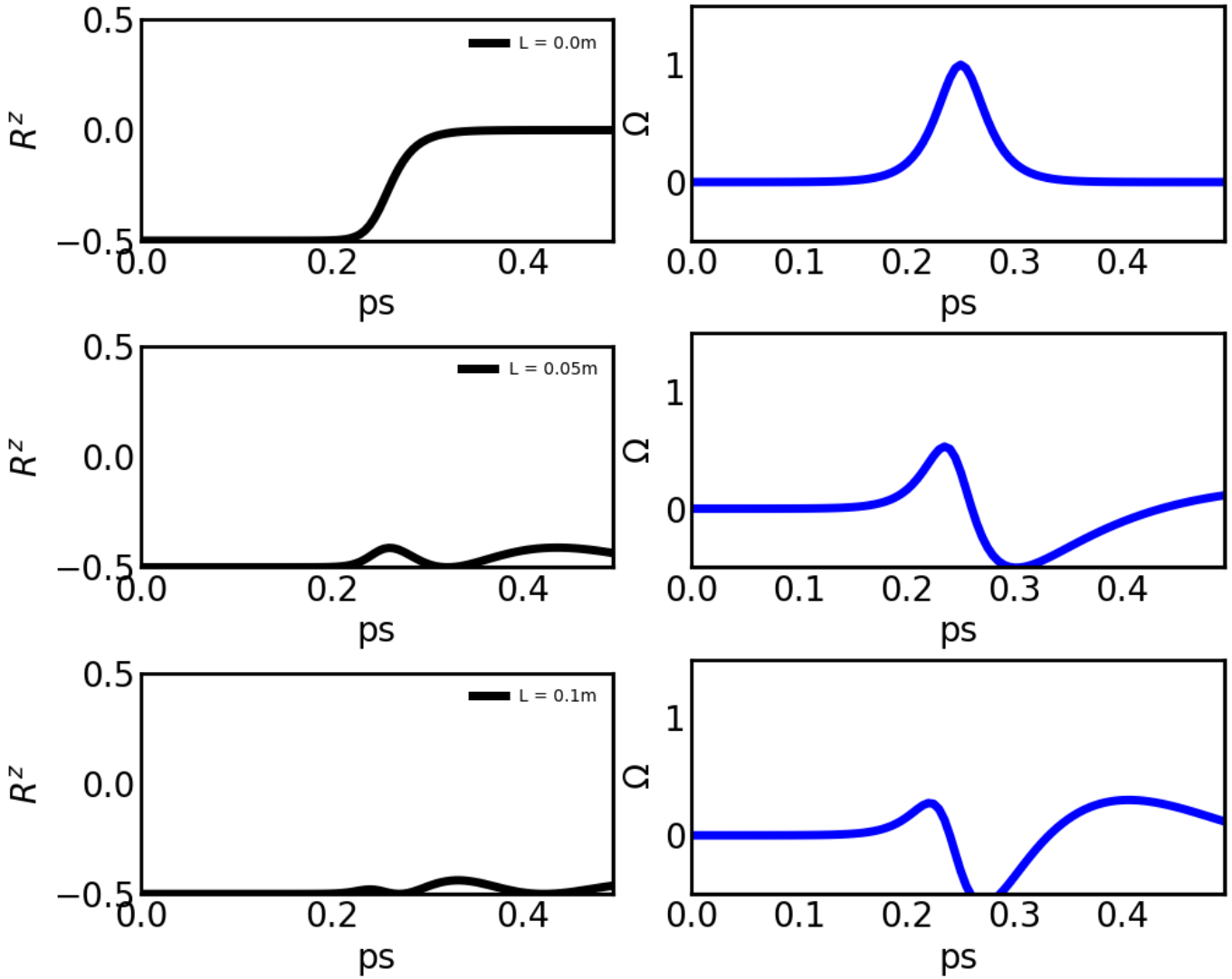

2π propagation

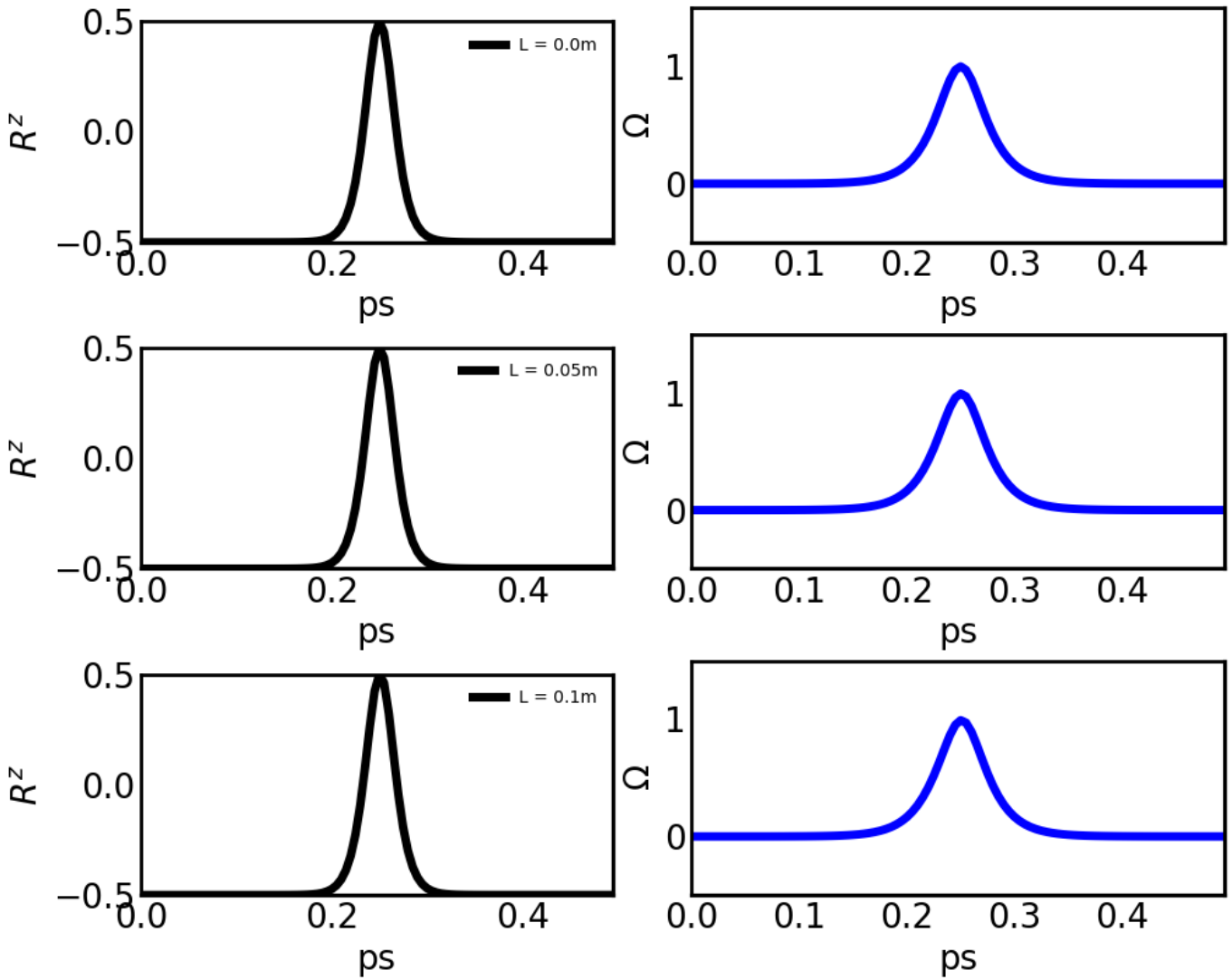

2.5π propagation

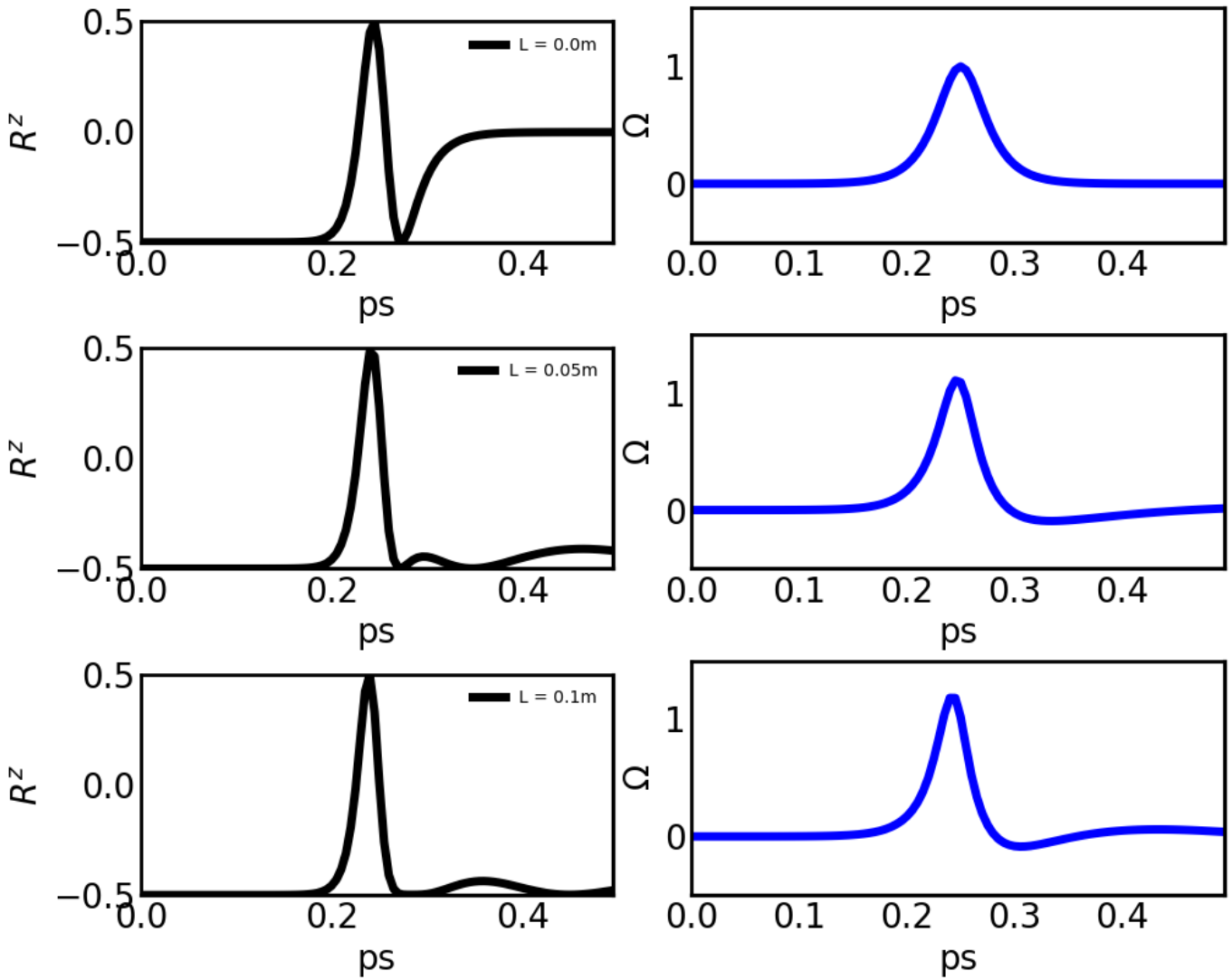

3.5π propagation

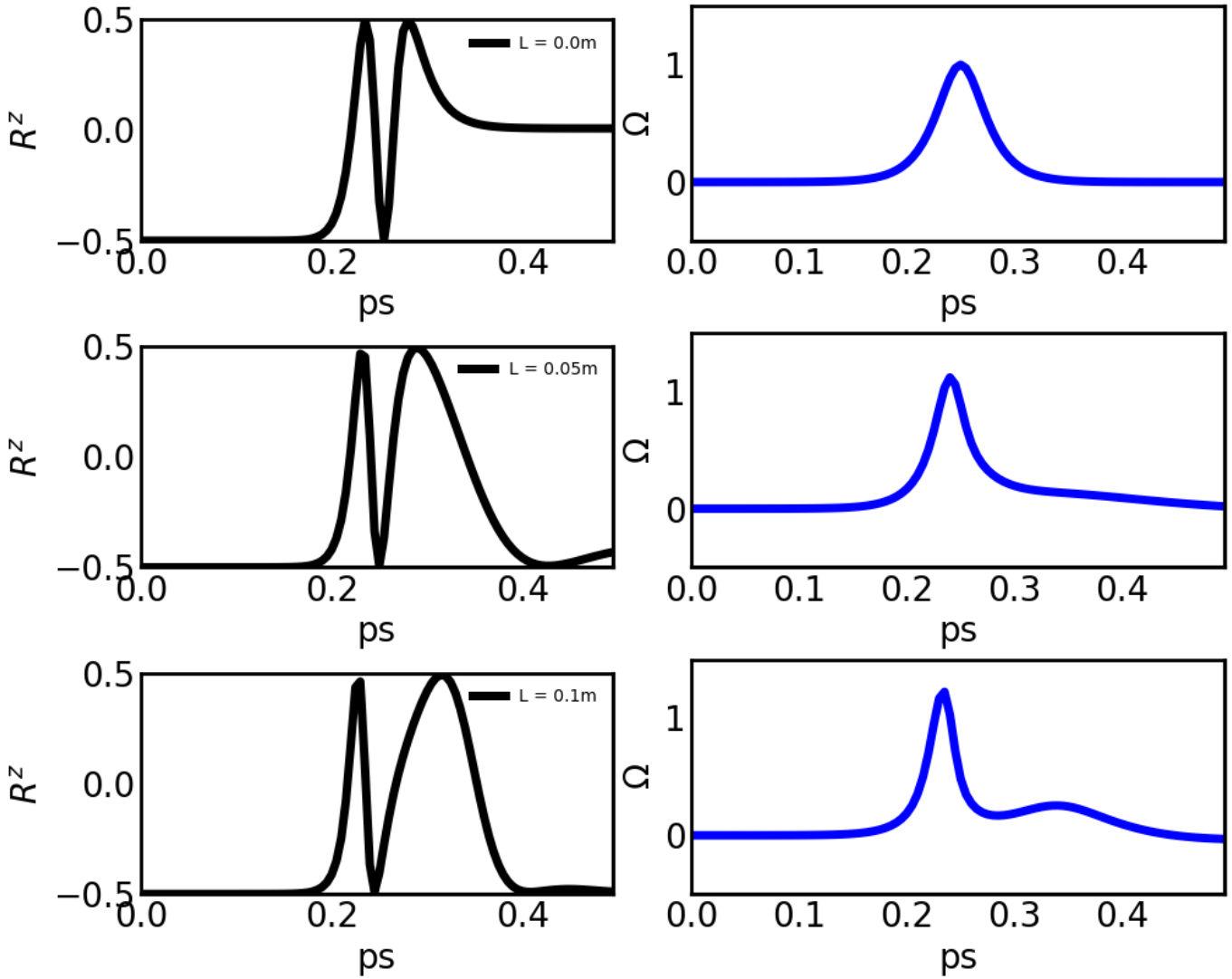

Area theorem

$$\frac{\mathbf{d}\theta}{\mathbf{dz}} = \frac{-\alpha}{\mathbf{2}} \sin(\theta),$$

α the linear optical attenuation coefficient

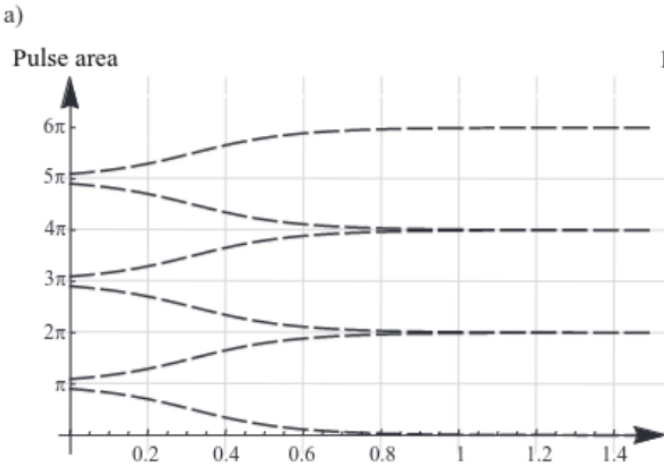

Pulse at resonance

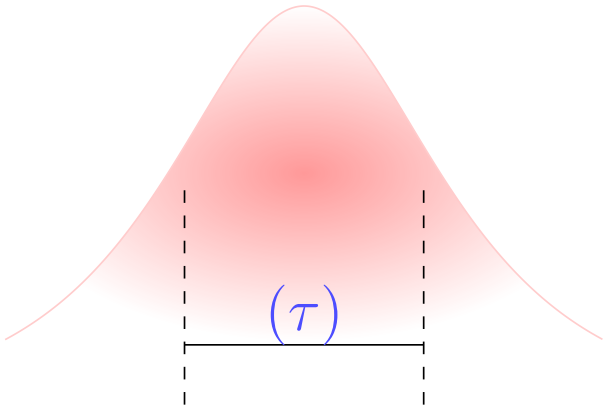

Resonant gas

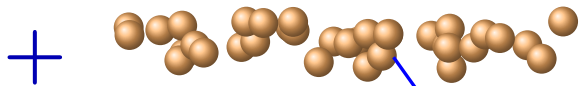

$+$ $=$???

lineshape of the resonant gas

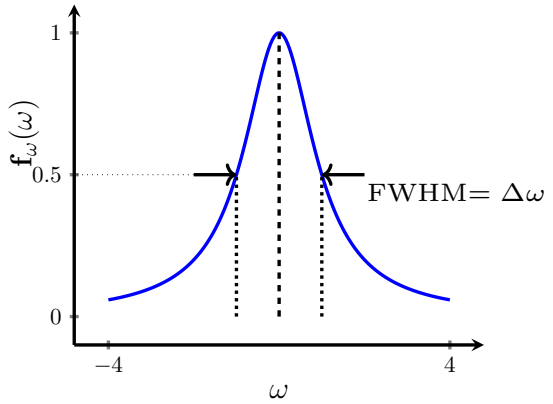

Pulse at resonance

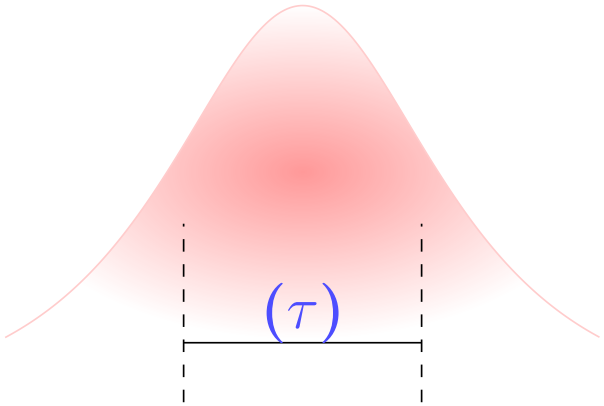

Resonant gas

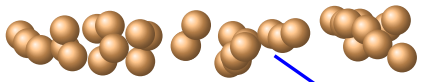

lineshape of the resonant gas

$+$ $=$ **SIT**

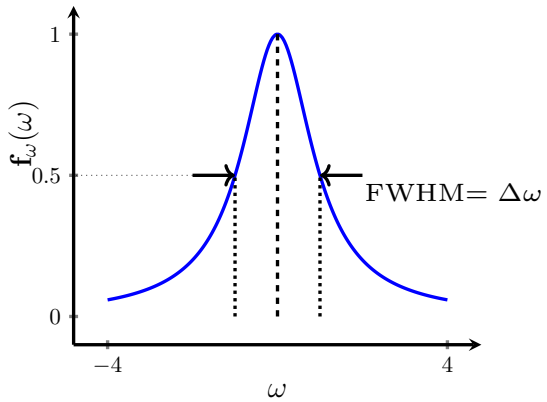

if $\tau < 1/\Delta\omega$ ⟶ Transparent ✓

Pulse at resonance

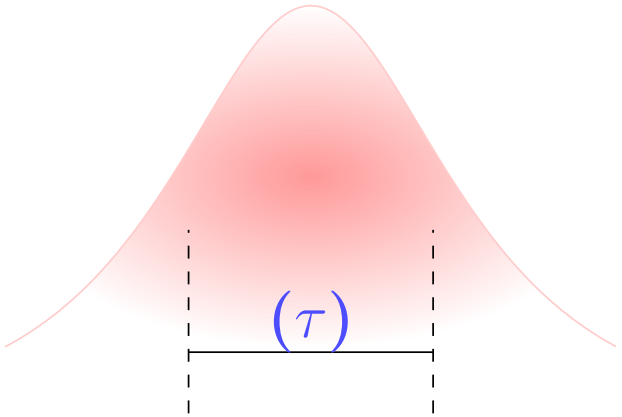

+

Resonant gas

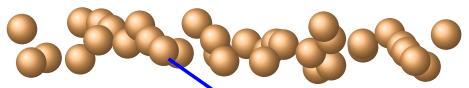

=

lineshape of the resonant gas

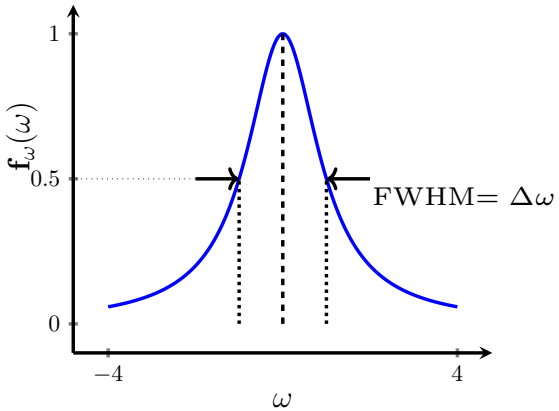

if $\tau > 1/\Delta\omega$ ⟶ Absorption ✗

two level atom

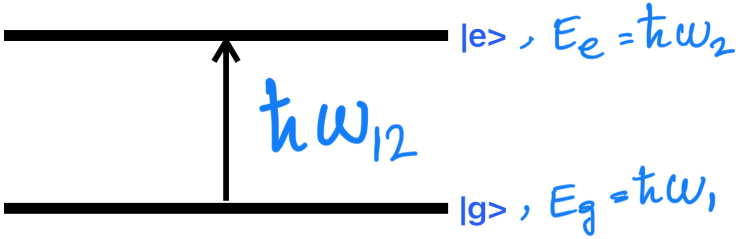

$$\hat{\mathbf{H}} = \hat{\mathbf{H}}_\mathbf{0} - \hat{\mathbf{d}} \cdot \hat{\mathbf{E}}(\mathbf{t})$$
$$\mathbf{E}(\mathbf{t}) = \varepsilon \mathbf{E}_\mathbf{0} \cos(\omega \mathbf{t})$$

where $\hat{d}$ is the dipole moment, ε is the polarization vector and E_0 amplitude of the light field with frequency ω.

The time dependent Schrödinger Eq;

$$\mathbf{i}\hbar\frac{\partial}{\partial \mathbf{t}}|\psi(\mathbf{t})\rangle = \hat{\mathbf{H}}|\psi(\mathbf{t})\rangle$$

We need stable relative phase between two states.

two level atom

But usually we have phase fluctuation due to state preparation.

We need a new formalism which allows us to describe mixed states.

(imperfect state preparation, spontaneous emission, damping, incoherent pumping, ...)

One way to describe this, is through density operator(matrix) formalism!

$$\hat{\rho} = \sum_i P_i |\psi_i\rangle\langle\psi_i|$$

$$\sum_i P_i = 1$$

Time evolution (von Neumann equation)

$$\mathbf{i}\hbar\frac{\partial\hat{\rho}}{\partial\mathbf{t}} = \left[\hat{\mathbf{H}}, \hat{\rho}\right]$$

The spectral lineshape function

The radiation emitted in atomic transition is not perfectly monochromatic.

The shape of the emission line is described by the spectrum lineshape function $g_\omega(\omega)$.

The function that peaks at the line center defined by

$$\hbar\omega_0 = (E_2 - E_1),$$

and is normalized $\int_0^\infty g_\omega(\omega)d\omega = 1$.

Full width at half maximum (FWHM) $\Delta\omega$

The main broadening mechanism that can occur in gases:

Lifetime (natural) broadening

Collisional (pressure) broadening

Doppler broadening

The medium is classified of the broadening mechanisms:

Homogeneous: all individual atoms produce the same spectrum, (**Lorentzian** lineshape),

inhomogeneous: all individual behave differently , produce (**Gaussian** spectral lines).

Lifetime broadening

Light is emitted when an electron in an excited state

drops to a lower level by spontaneous emission rate

Einstein A coefficient = spontaneous emission rate,

the radiative lifetime $\tau = \frac{ln(2)}{\gamma_0}$

The finite lifetime of the excited state $\rightarrow$ broadening of the spectral line

accordance with the energy time uncertainty principle

$$\Delta E \Delta t \geq \hbar,\ \Delta t = \tau,\ \Delta\omega \geq \frac{1}{\tau}$$

$$g_\omega(\omega) = \frac{\Delta\omega}{2\pi} \frac{1}{(\omega-\omega_0)^2+(\Delta\omega/2)^2}$$

where the FWHM is given by :

$$\Delta\omega_{lifetime} = \frac{1}{\tau}$$

Collisional (pressure) broadening

collision between atoms in gas $\rightarrow$
shorten the effective lifetime of the excited state

if the mean time between collisons $\tau_{collision} \leq \tau$ (radiative life time)

leads to additional line broadening

$$\tau_{collison} \sim \frac{1}{\sigma_s P}\left(\frac{\pi m k_B T}{8}\right)^{1/2}$$

where σ_s is collision cross section,
P is the pressure and T is the temperature.

Doppler broadening

Gaussian lineshape function

$$g_\omega(\omega) = \frac{c}{\omega_0}\sqrt{\frac{m}{2\pi k_B T}}\exp\left(-\frac{mc^2(\omega-\omega_0)^2}{2k_B T\omega_0^2}\right)$$

with a FWHM given by

$$\Delta\omega_{Doppler} = 2\omega_0\left(\frac{(2ln(2))k_B T}{mc^2}\right)^{1/2} = \frac{4\pi}{\lambda}\left(\frac{(2ln2)k_B T}{m}\right)^{1/2}$$

The main broadening mechanism that can occur in gases:

- Lifetime (natural) broadening ✓
- Collisional (pressure) broadening ✗
- Doppler broadening ✓

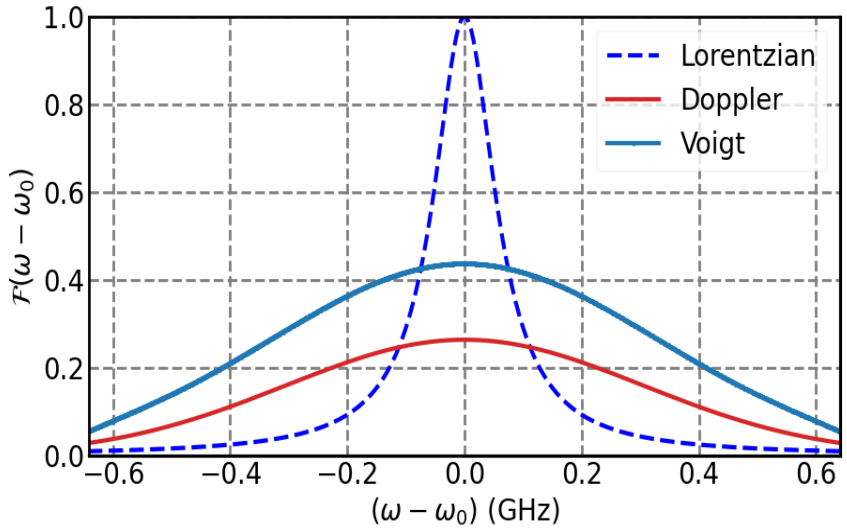

Coherent state

$(\Delta X_1\ \Delta X_2 \geq \frac{1}{4}),[X_1, X_2] \neq 0$

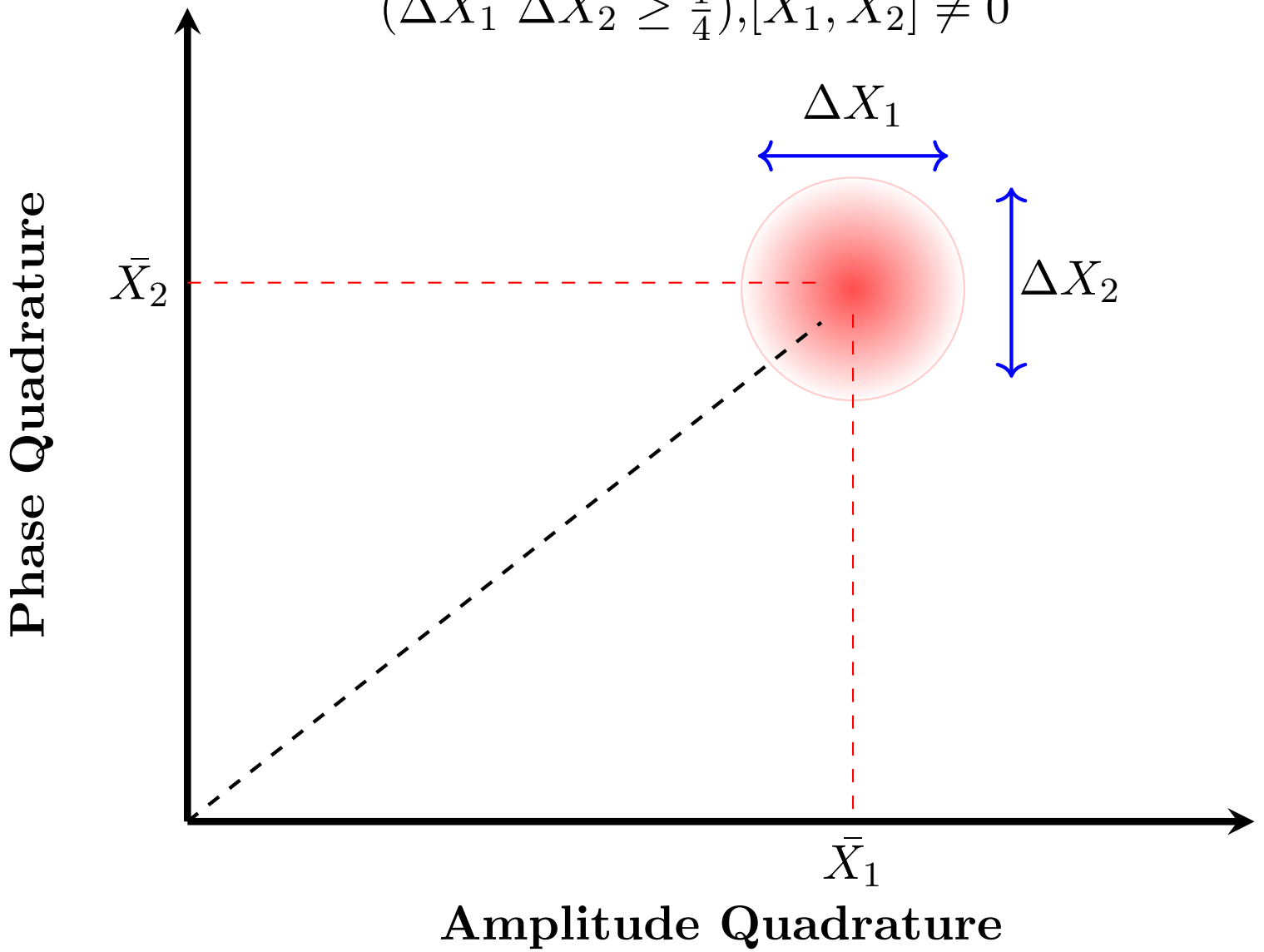

Squeezed state

$(\Delta X_\theta < 1/2)$

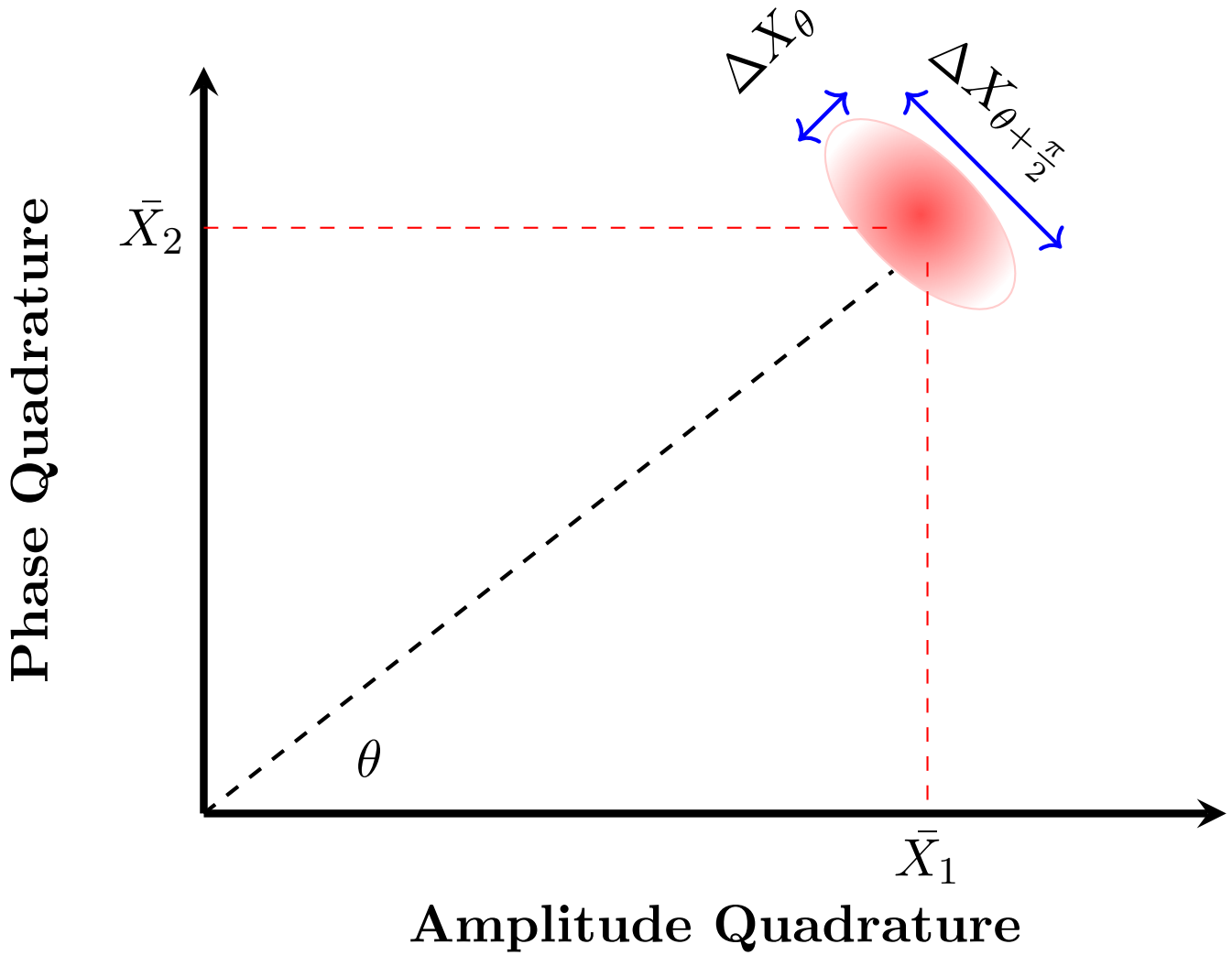

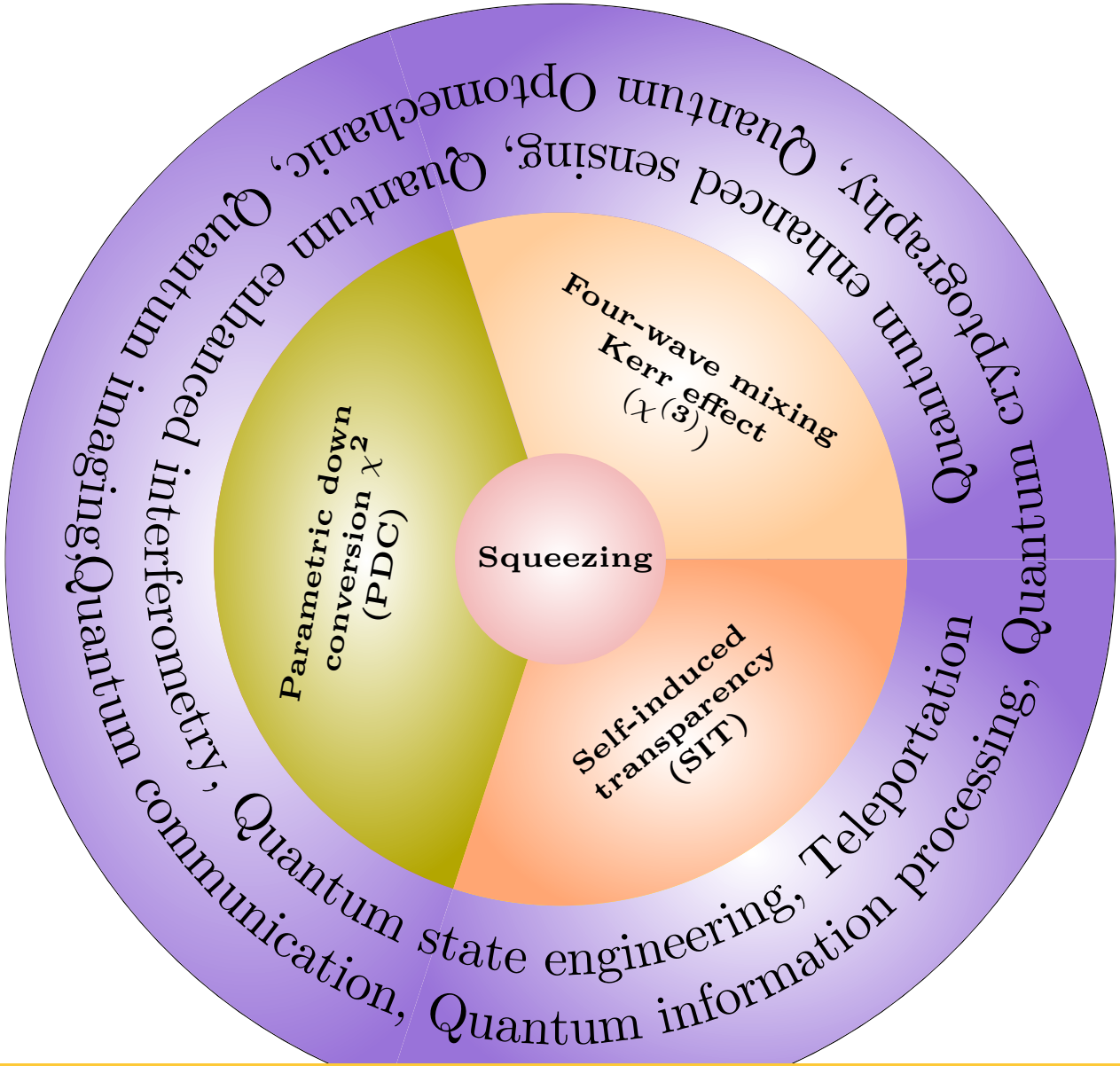
Quantum enhanced sensing, Quantum Optomechanic, Quantum cryptography, Quantum information processing, Quantum state engineering, Teleportation
Quantum enhanced interferometry, Quantum communication, Quantum imaging,Quantum
Squeezing
Parametric down conversion χ^2 (PDC)
Four-wave mixing Kerr effect $(\chi^{(3)})$
Self-induced transparency (SIT)

Model

$$\hat{H}_0 = \hat{H}_\mathrm{A} + \hat{H}_\mathrm{F} + \hat{H}_\mathrm{B}$$

$$= \sum_\mu \tfrac{1}{2}\hbar\omega_\mu \hat{\sigma}_\mu^z + \hbar\omega \hat{a}^\dagger \hat{a} + \sum_k \hbar\omega_k \hat{b}_k^\dagger \hat{b}_k$$

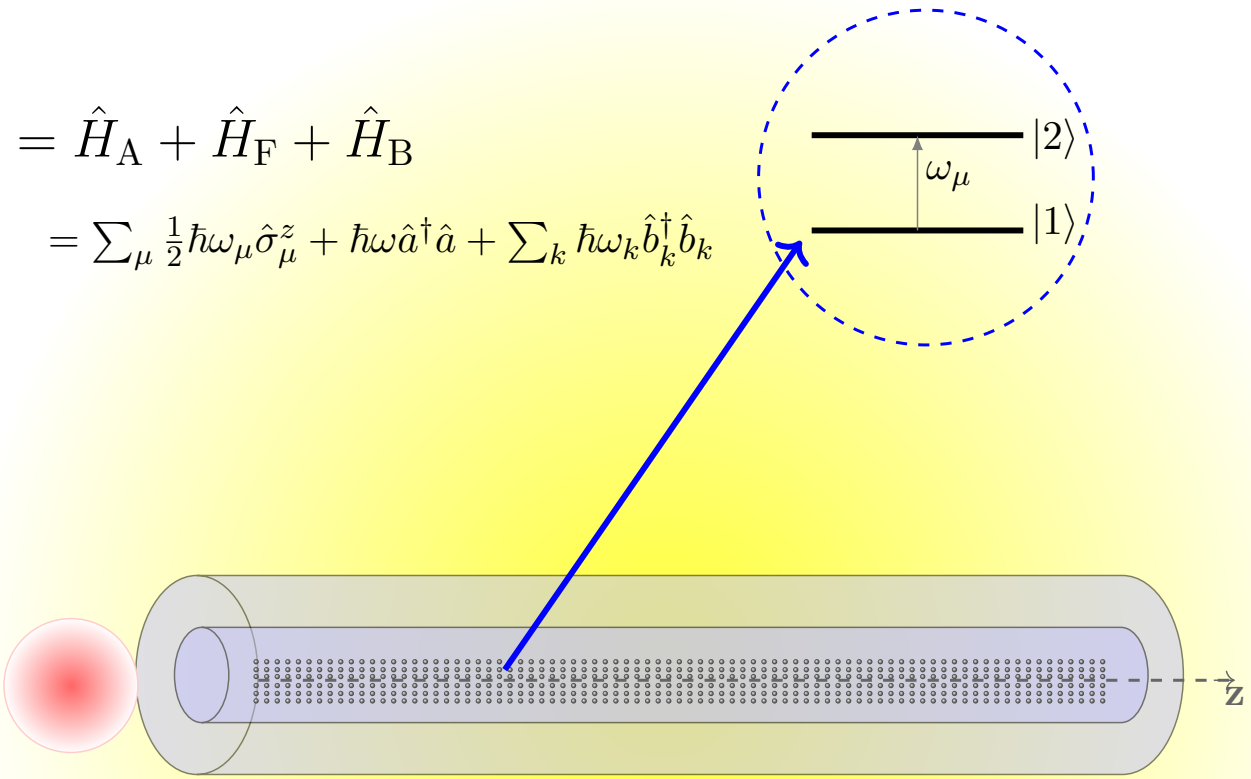

$$\hat{H}_I = \hat{H}_\mathrm{AB} + \hat{H}_\mathrm{FB} + \hat{H}_\mathrm{AF}$$

$$= \hbar\sum_\mu (\hat{\Gamma}_\mu^{\sigma\dagger}\hat{\sigma}_\mu^- + \hat{\Gamma}_\mu^{\sigma}\hat{\sigma}_\mu^+ + \hat{\Gamma}_\mu^{\sigma}\hat{\sigma}_\mu^z) + \hbar(\hat{\Gamma}^{a\dagger}\hat{a} + \hat{\Gamma}^{a}\hat{a}^\dagger) + \hbar\sum_\mu (g\hat{a}^\dagger\hat{\sigma}_\mu^- e^{-ik\cdot x_\mu} + \mathrm{H.c.})$$

$$\frac{\partial\hat{\rho}}{\partial \mathbf{t}} = \frac{\mathbf{1}}{\mathbf{i}\hbar}[\hat{\mathbf{H}}_{\mathbf{int}}, \hat{\rho}] + (\frac{\partial\hat{\rho}}{\partial \mathbf{t}})_{\mathbf{field}} + (\frac{\partial\hat{\rho}}{\partial \mathbf{t}})_{\mathbf{atoms}}$$

$$\left[-\mathbf{i}(\omega-\omega_{\mathbf{0}})\hat{\mathbf{a}}^{\dagger}\hat{\mathbf{a}}, \hat{\rho}\right] + \left[-\mathbf{i}\sum_{\mu}(\omega_{\mu}-\omega_{\mathbf{0}})\hat{\sigma}_{\mu}^{\mathbf{z}}, \hat{\rho}\right] + \left[-\mathbf{ig}'\hat{\mathbf{a}}^{\dagger}\sum_{\mu}\hat{\sigma}_{\mu}^{-} + \mathbf{H.C}, \hat{\rho}\right]$$

$$\frac{\mathbf{W_{21}}}{\mathbf{2}}\sum_{\mu}\left(\left[\hat{\sigma}_{\mu}^{-}\hat{\rho}, \hat{\sigma}_{\mu}^{+}\right] + \left[\hat{\sigma}_{\mu}^{-}, \hat{\rho}\sigma_{\mu}^{+}\right]\right) + \frac{\mathbf{W_{12}}}{\mathbf{2}}\left(\left[\sigma_{\mu}^{+}\hat{\rho}, \hat{\sigma}_{\mu}^{-}\right] + \left[\sigma_{\mu}^{+}, \hat{\rho}\hat{\sigma}_{\mu}^{-}\right]\right) + \frac{\gamma_{\mathbf{p}}}{\mathbf{4}}\sum_{\mu}\left(\left[\hat{\sigma}_{\mu}^{\mathbf{z}}, \hat{\rho}\hat{\sigma}_{\mu}^{\mathbf{z}}\right] + \left[\hat{\sigma}_{\mu}^{\mathbf{z}}\hat{\rho}, \hat{\sigma}_{\mu}^{\mathbf{z}}\right]\right)$$

$$\frac{\mathbf{c}\kappa}{\mathbf{2}}\left(\mathbf{1}+\overline{\mathbf{n}}\right)\left(\left[\hat{\mathbf{a}}\hat{\rho}, \hat{\mathbf{a}}^{\dagger}\right] + \left[\hat{\mathbf{a}}, \hat{\rho}\hat{\mathbf{a}}^{\dagger}\right]\right) + \overline{\mathbf{n}}\left(\left[\hat{\mathbf{a}}^{\dagger}\hat{\rho}, \hat{\mathbf{a}}\right] + \left[\hat{\mathbf{a}}^{\dagger}, \hat{\rho}\hat{\mathbf{a}}\right]\right).$$

$W_{21} = \gamma_0(1+n)$, relaxation rate
$W_{12} = \gamma_0(n)$, incoherent pumping
$\gamma_P = 3\gamma_0$, dephasing

Hilbert space

The size of the Hilbert space grows exponentially with the size of the system.

The density matrix, which describes the statistical state of a quantum system, also grows exponentially in size as the system becomes larger. For example:

For a single qubit, the density matrix is a 2×2 matrix: $\begin{pmatrix} \rho_{00} & \rho_{01} \\ \rho_{10} & \rho_{11} \end{pmatrix}$

For a N=2 , the density matrix is a 4×4 matrix: $\begin{pmatrix} \rho_{00} & \rho_{01} & \rho_{02} & \rho_{03} \\ \rho_{10} & \rho_{11} & \rho_{12} & \rho_{13} \\ \rho_{20} & \rho_{21} & \rho_{22} & \rho_{23} \\ \rho_{30} & \rho_{31} & \rho_{32} & \rho_{33} \end{pmatrix}$

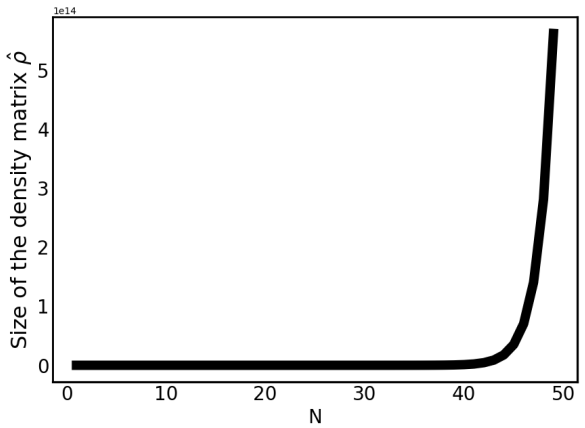

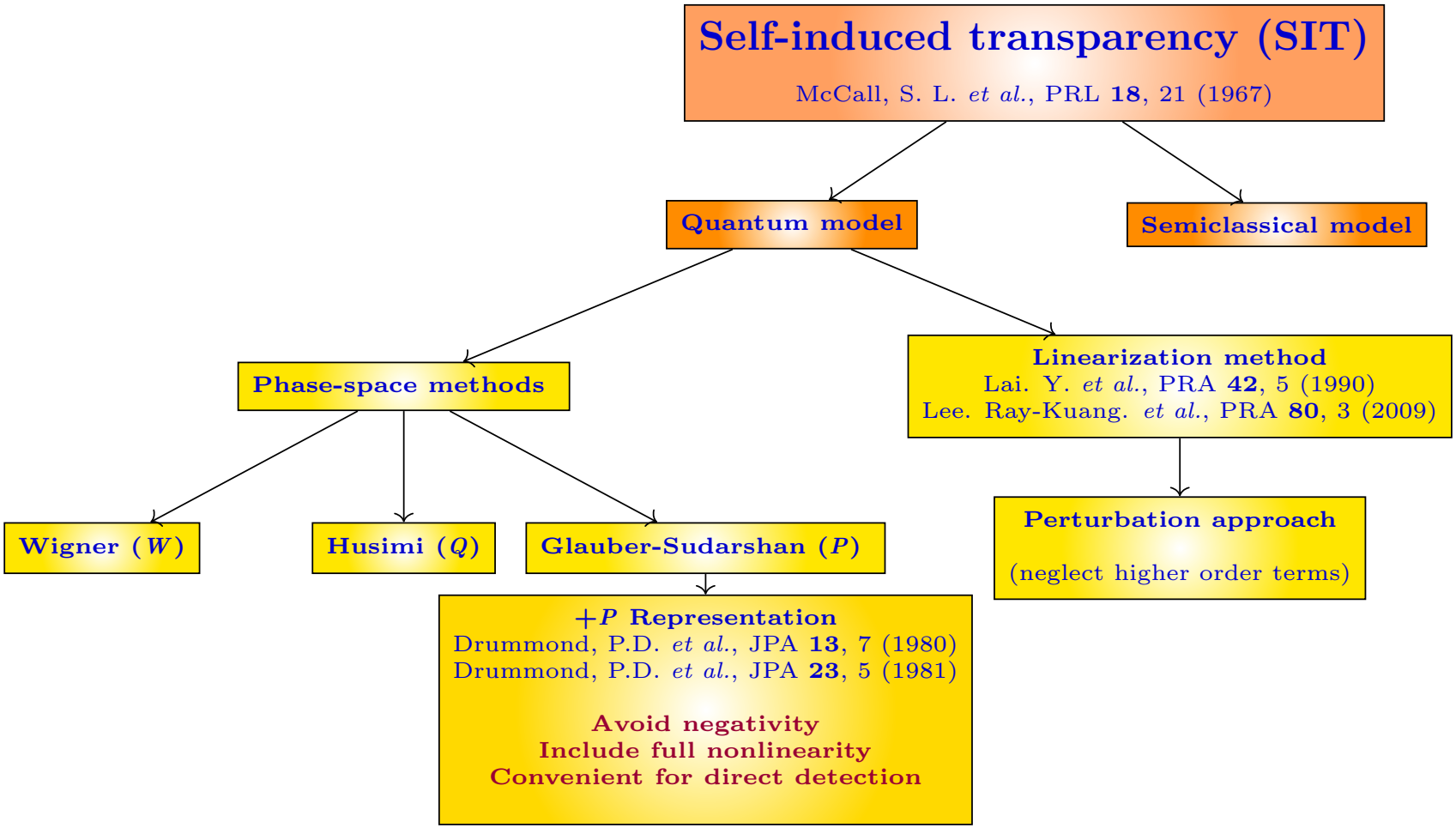
Self-induced transparency (SIT)
McCall, S. L. et al., PRL 18, 21 (1967)
Quantum model
Semiclassical model
Phase-space methods
Linearization method
Lai. Y. et al., PRA 42, 5 (1990)
Lee. Ray-Kuang. et al., PRA 80, 3 (2009)
Wigner (W)
Husimi (Q)
Glauber-Sudarshan (P)
Perturbation approach
(neglect higher order terms)
+P Representation
Drummond, P.D. et al., JPA 13, 7 (1980)
Drummond, P.D. et al., JPA 23, 5 (1981)
Avoid negativity
Include full nonlinearity
Convenient for direct detection

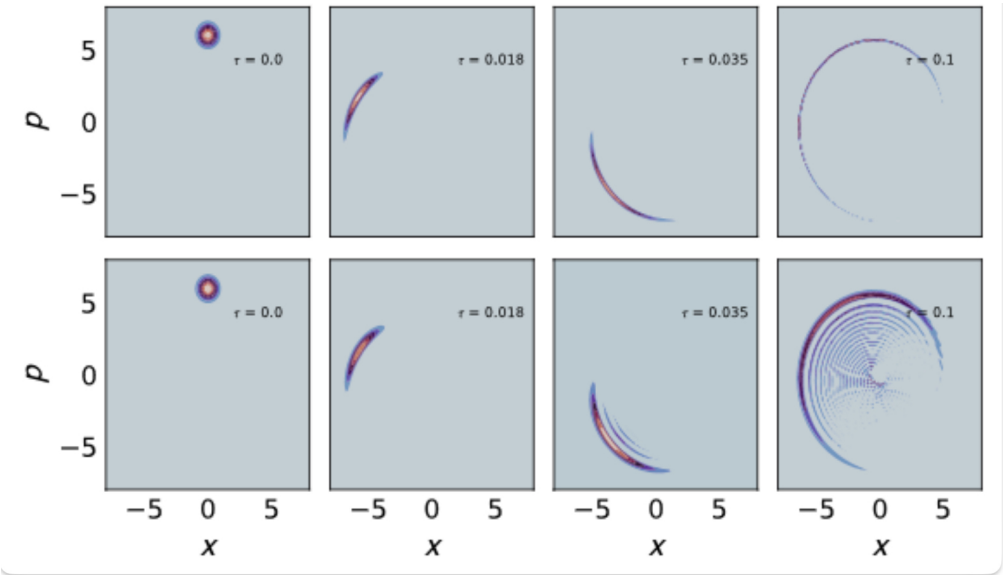

Optics Communications 545 (2023) 129717

Contents lists available at ScienceDirect

Optics Communications

journal homepage: www.elsevier.com/locate/optcom

Quasiclassical approach to the nonlinear Kerr dynamics

Mojdeh S. Najafabadi [a], Andrei B. Klimov [b], Luis L. Sánchez-Soto [a,c,*], Gerd Leuchs [a,d]

[a] Max–Planck-Institut für die Physik des Lichts, Erlangen, 91058, Germany
[b] Departamento de Física, Universidad de Guadalajara, Guadalajara, 44420, Jalisco, Mexico
[c] Departamento de Optica, Universidad Complutense, Madrid, 28040, Spain
[d] Institut fur Optik, Information und Photonik, Friedrich-Alexander-Universität Erlangen-Nürnberg, Erlangen, 91058, Germany

$$\frac{\partial\hat{\rho}}{\partial \mathbf{t}} = \frac{\mathbf{1}}{\mathbf{i}\hbar}[\hat{\mathbf{H}}_{\mathbf{int}}, \hat{\rho}] + (\frac{\partial\hat{\rho}}{\partial \mathbf{t}})_{\mathbf{field}} + (\frac{\partial\hat{\rho}}{\partial \mathbf{t}})_{\mathbf{atoms}}$$

$$\left[-\mathbf{i}(\omega-\omega_{\mathbf{0}})\hat{\mathbf{a}}^{\dagger}\hat{\mathbf{a}}, \hat{\rho}\right] + \left[-\mathbf{i}\sum_{\mu}(\omega_{\mu}-\omega_{\mathbf{0}})\hat{\sigma}_{\mu}^{\mathbf{z}}, \hat{\rho}\right] + \left[-\mathbf{ig}'\hat{\mathbf{a}}^{\dagger}\sum_{\mu}\hat{\sigma}_{\mu}^{-} + \mathbf{H.C}, \hat{\rho}\right]$$

$$\frac{\mathbf{W_{21}}}{\mathbf{2}}\sum_{\mu}\left(\left[\hat{\sigma}_{\mu}^{-}\hat{\rho}, \hat{\sigma}_{\mu}^{+}\right] + \left[\hat{\sigma}_{\mu}^{-}, \hat{\rho}\sigma_{\mu}^{+}\right]\right) + \frac{\mathbf{W_{12}}}{\mathbf{2}}\left(\left[\sigma_{\mu}^{+}\hat{\rho}, \hat{\sigma}_{\mu}^{-}\right] + \left[\sigma_{\mu}^{+}, \hat{\rho}\hat{\sigma}_{\mu}^{-}\right]\right) + \frac{\gamma_{\mathbf{p}}}{\mathbf{4}}\sum_{\mu}\left(\left[\hat{\sigma}_{\mu}^{\mathbf{z}}, \hat{\rho}\hat{\sigma}_{\mu}^{\mathbf{z}}\right] + \left[\hat{\sigma}_{\mu}^{\mathbf{z}}\hat{\rho}, \hat{\sigma}_{\mu}^{\mathbf{z}}\right]\right)$$

$$\frac{\mathbf{c}\kappa}{\mathbf{2}}\left(\mathbf{1}+\overline{\mathbf{n}}\right)\left(\left[\hat{\mathbf{a}}\hat{\rho}, \hat{\mathbf{a}}^{\dagger}\right] + \left[\hat{\mathbf{a}}, \hat{\rho}\hat{\mathbf{a}}^{\dagger}\right]\right) + \overline{\mathbf{n}}\left(\left[\hat{\mathbf{a}}^{\dagger}\hat{\rho}, \hat{\mathbf{a}}\right] + \left[\hat{\mathbf{a}}^{\dagger}, \hat{\rho}\hat{\mathbf{a}}\right]\right).$$

$W_{21} = \gamma_0(1+n)$, relaxation rate
$W_{12} = \gamma_0(n)$, incoherent pumping
$\gamma_P = 3\gamma_0$, dephasing

Drummond. P.D. et al., PRA **44**, 3 (1991)

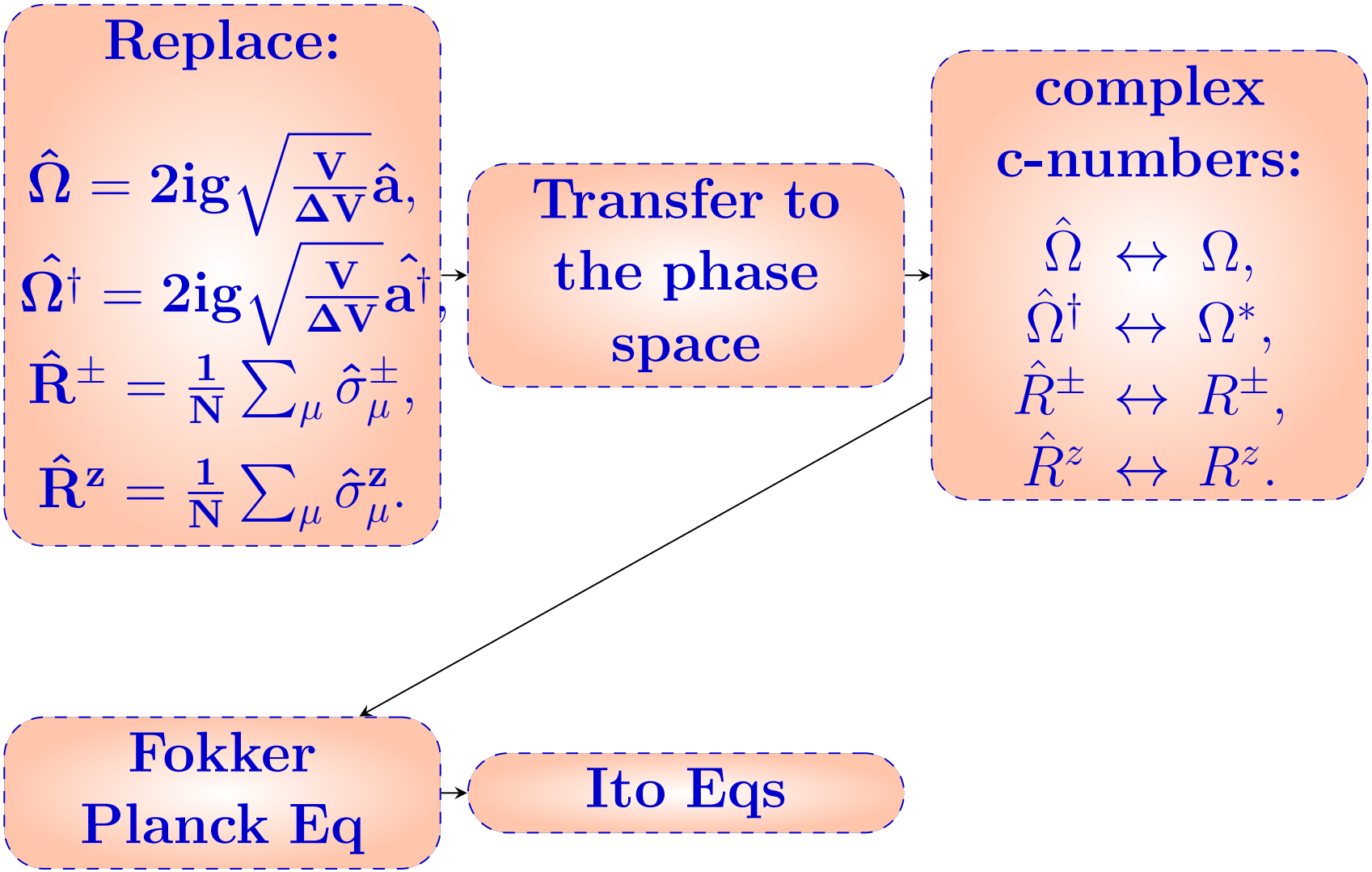

$$\left(\frac{\partial}{\partial z}+(\frac{1}{c}-\frac{1}{v_g})\frac{\partial}{\partial \tau}\right)\Omega(\tau,z)=-\frac{1}{2}\kappa\Omega(\tau,z)+G\int\rho(z,\omega)R^{-}(\tau,z,\omega)d\omega$$
$$+F^{\Omega}(\tau,z),$$

$$\frac{\partial}{\partial \tau}R^{\pm}(\tau,z,\omega)=-(\gamma_{\perp}\pm i(\omega-\omega_0))R^{\pm}(\tau,z,\omega)+\Omega(\tau,z)R^{z}(\tau,z,\omega)$$
$$+F^{R}(\tau,z,\omega),$$

$$\frac{\partial}{\partial \tau}R^{z}(\tau,z,\omega)=-\gamma_{\parallel}\left[R^{z}(\tau,z,\omega)-\sigma^{SS}\right]-\frac{1}{2}\Big[\Omega(\tau,z)R^{+}(\tau,z,\omega)$$
$$+\Omega^{\dagger}(\tau,z)R^{-}(\tau,z,\omega)\Big]+F^{z}(\tau,z,\omega),$$

$$2\xi_j^{\alpha}(z_j)\sqrt{G\kappa\overline{n}/dz}$$

$$\left(\frac{\partial}{\partial z}+\left(\frac{1}{c}-\frac{1}{v_g}\right)\frac{\partial}{\partial \tau}\right)\Omega_j(\tau,z)=-\frac{1}{2}\kappa\Omega_j(\tau,z)+G\int\rho_j(z,\omega)R_j^{-}(\tau,z,\omega)d\omega$$
$$+F_n^{\Omega}(\tau,z),$$

$$\frac{\partial}{\partial\tau}R_n^{\pm}(\tau,z,\omega)=-(\gamma_{\perp}\pm i(\omega-\omega_0))R_n^{\pm}(\tau,z,\omega)+\Omega(\tau,z)R_n^{z}(\tau,z,\omega)$$
$$+F_n^{R}(\tau,z,\omega),$$

$$\xi_{\mathrm{n}}^{J}(\tau)\sqrt{2\Omega R_n^{-}/N_{\mathrm{n}}}$$
$$+2\xi_{\mathrm{n}}^{P}(\tau)\sqrt{\gamma_P(R_n^{z}+1)/N_{\mathrm{n}}}$$
$$+2\xi_{\mathrm{n}}^{o}(\tau)\sqrt{W_{12}/N_{\mathrm{n}}}$$

$$\frac{\partial}{\partial\tau}R_n^{z}(\tau,z,\omega)=-\gamma_{\parallel}\left[R_n^{z}(\tau,z,\omega)-\sigma^{SS}\right]-\frac{1}{2}\Big[\Omega(\tau,z)R_n^{+}(\tau,z,\omega)$$
$$+\Omega^{\dagger}(\tau,z)R_n^{-}(\tau,z,\omega)\Big]+F_n^{z}(\tau,z,\omega),$$

$$\xi_{\mathrm{n}}^{z}(\tau)\Bigg[(2\gamma_{\parallel})(1-\sigma^{SS}R_n^{z})$$
$$+\frac{(R_n^{-}\Omega^{\dagger}-R_n^{+}\Omega)-2W_{12}R_n^{+}R_n^{-}}{N_{\mathrm{n}}}\Bigg]^{1/2}$$
$$-\Big[\xi_{\mathrm{n}}^{o}(\tau)R_n^{+}+\xi_{\mathrm{n}}^{o*}(\tau)R_n^{-}\Big]$$
$$\sqrt{W_{12}/N_{\mathrm{n}}}$$

$$\langle\xi^{\alpha}(z)\xi^{\alpha*}(z')\rangle=\delta(z-z'),$$
$$\langle\xi_{\mathrm{n}}^{o}(\tau)\xi_{\mathrm{n}'}^{o*}(\tau')\rangle=\delta(\tau-\tau')\delta^2_{\mathrm{n},\mathrm{n}'}$$

$$\langle\xi_{\mathrm{n}}^{P}(\tau)\xi_{\mathrm{n}'}^{P*}(\tau')\rangle=\delta(\tau-\tau')\delta^2_{\mathrm{n},\mathrm{n}'},$$
$$\langle\xi_{\mathrm{n}}^{J}(\tau)\xi_{\mathrm{n}'}^{J}(\tau')\rangle=\delta(\tau-\tau')\delta^2_{\mathrm{n},\mathrm{n}'}$$

$$\langle\xi_{\mathrm{n}}^{z}(\tau)\xi_{\mathrm{n}'}^{z}(\tau')\rangle=\delta(\tau-\tau')\delta^2_{\mathrm{n},\mathrm{n}'}$$

The initial conditions

$\mathrm{P}(\tau, \mathbf{\Omega}, \mathbf{\Omega}^\dagger) = \delta^{(2)}(\mathbf{\Omega}^* - \mathbf{\Omega}^\dagger)\delta^{(2)}(\mathbf{\Omega} - \mathbf{\Omega}(\mathbf{0}, \tau))$, $\rightarrow$ $(\mathbf{\Omega}^\dagger, \mathbf{\Omega})$ Rabi frequency

$\mathbf{\Omega}(\mathbf{0}, \tau) = 2A \ \mathrm{sech}\left[A(\tau - \tau_0)\right] \exp(i(\delta\tau + \phi(z))$,

$\mathrm{P}(\mathbf{R}) = \delta^{(2)}(\mathbf{R}^+)\delta^{(2)}(\mathbf{R}^-)\delta^{(2)}(\mathbf{R^z} + 1/2)$.$\rightarrow$ $(\mathbf{R}^\pm, \mathbf{R^z})$ Bloch vectors

Direct detection $\hat{\mathrm{M}}(z) = \int_{-\infty}^{\infty} \hat{\mathbf{\Omega}}^{\dagger}(\tau, z)\hat{\mathbf{\Omega}}(\tau, z)d\tau,$

$$S = 10\log_{10}\left(1 + \frac{\mathrm{var}_{+P}(M)}{<\hat{M}>}\right)$$

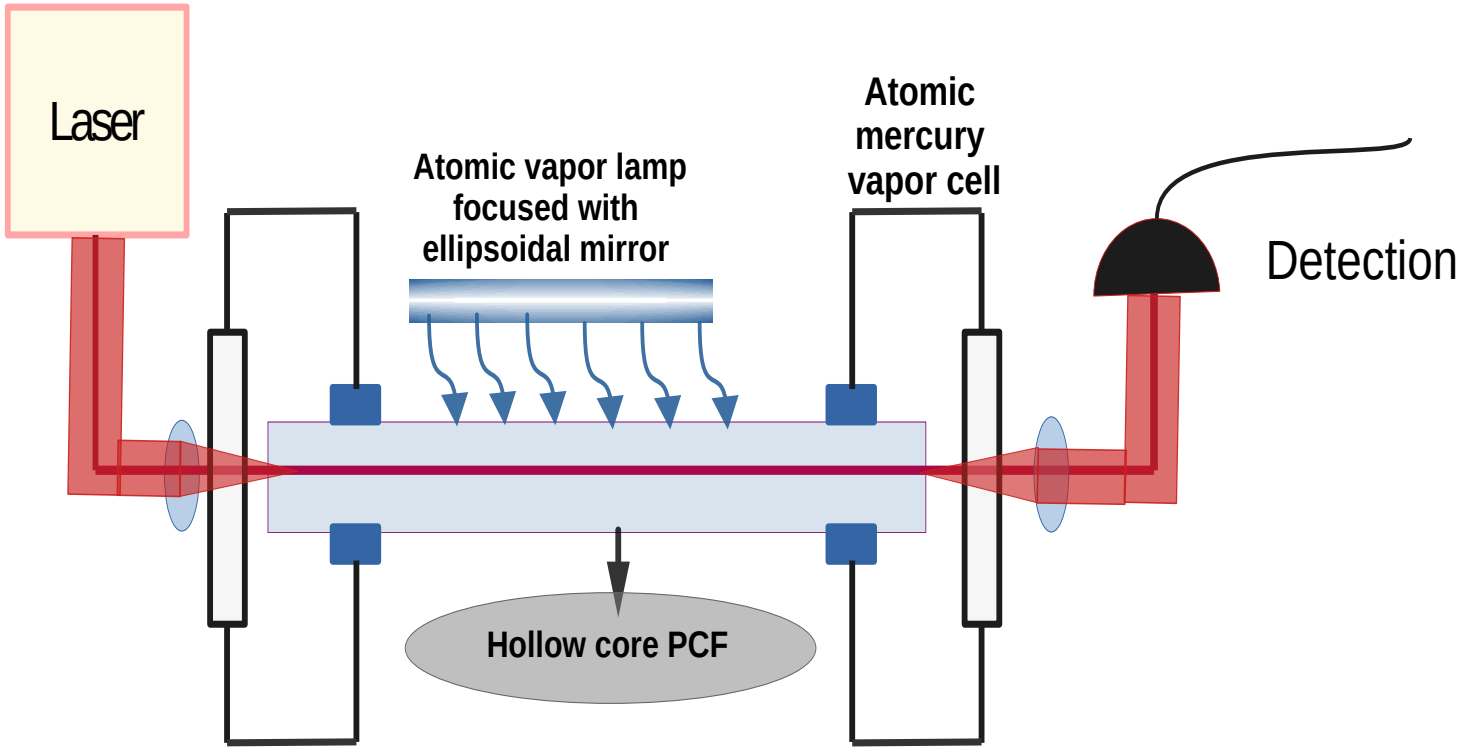

Amplitude squeezing

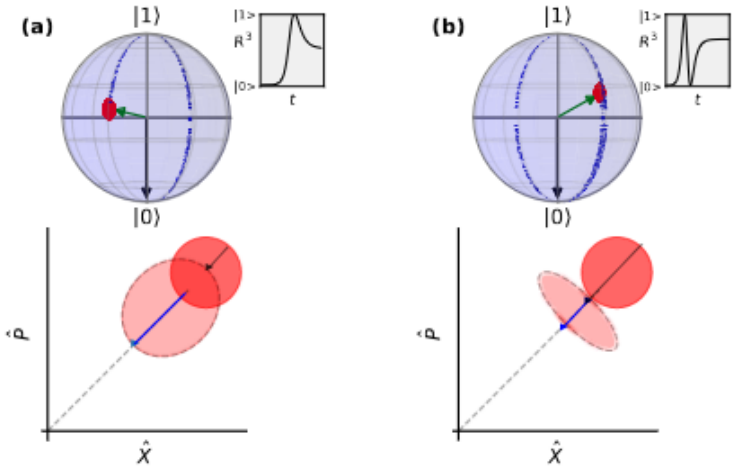

FIG. 3. At the top, we show the atomic evolution as both, a trajectory of the Bloch vector and as the time evolution of the population inversion (gray inset). At the bottom the phase-space representation of the excitation of the pulse is shown: the coherent state before the interaction (red) and the distorted state after the interaction (pink). In (a) the initial pulse area is less than 2π and in (b) the pulse area is larger than 2π. The atomic excitation left behind corresponds to an attenuation of the light pulse. In (a) larger amplitudes within the uncertainty region are attenuated less than lower amplitudes resulting in increased amplitude uncertainty. In (b) the roles are reversed: larger amplitudes are attenuated more than lower ones, leading to squeezing of the amplitude uncertainty.

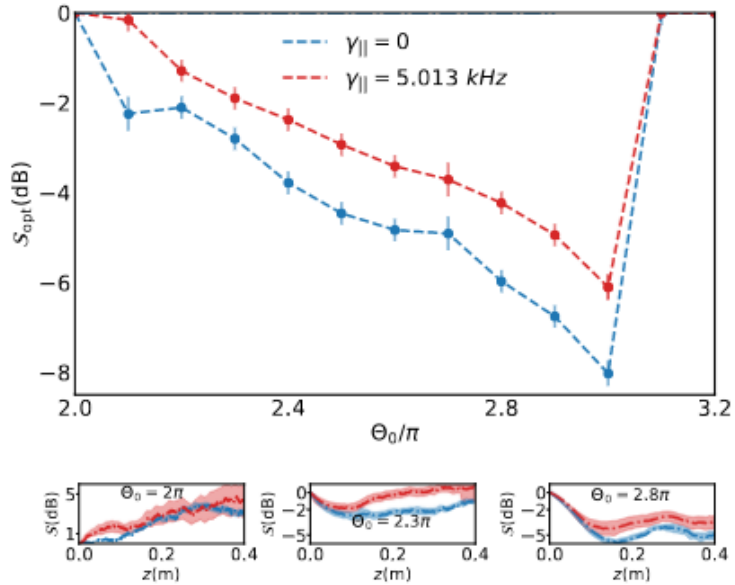

FIG. 4. Optimum squeezing as a function of the initial area of the input pulse in the presence and absence of longitudinal damping. The bottom subplots indicate the evolution of squeezing for pulses with the initial area 2π, 2.3π, and 2.8π. The blue curves are in the absence of the longitudinal damping while the red curves capture the effect of the damping. The transparent shaded color shows the uncertainty of the achieved squeezing from 4000 samples in each grid point. The longitudinal damping rate is taken to be $\gamma_{\parallel} = 5.013kHz$, while temperature is kept to zero. The pulse duration $\tau = 99.97$ ns and the atomic properties are the same as in Fig. 2.

Phys. Rev. Research **6**, 023142

Experiment

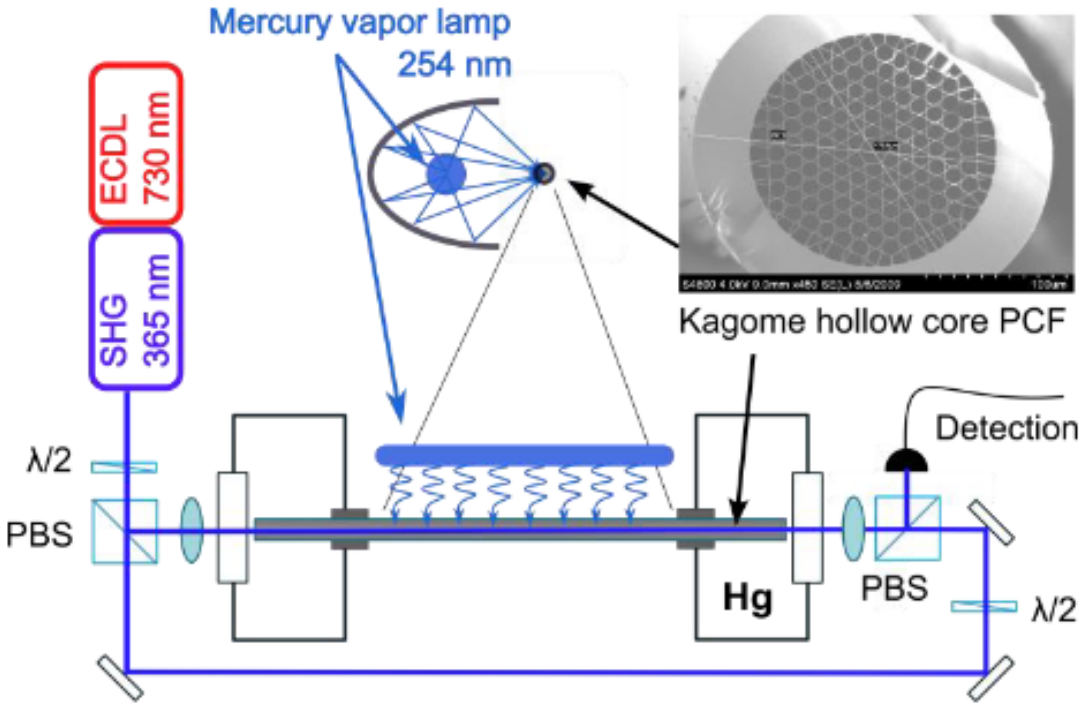

Fig. 1. Experimental set-up. The mercury vapor in the hollow-core PCF is pumped incoherently from the side by a mercury vapor lamp (main wavelength 254 nm, with significant contributions at 405 nm, 436 nm, and 546 nm), which populates the 6^3P_2 level. The 6^3P_2 - 6^3D_3 transition is probed with frequency-doubled light from a diode laser.

Vogl, U. et al., Opt 22, 24 (2014)

Hyperfine structure for the $6^3D_3 \rightarrow 6^3P_2$ 3650 Å line of natural Hg

Isotope mass No.	**I**	**Abundance** (%)	**transition** $F(^3D_3) \rightarrow F(^3D_3)$
196	0	0.15	3→ 2
198	0	10.02	3→ 2
200	0	23.13	3→ 2
202	0	29.80	3→ 2
204	0	6.85	3→ 2
199	$\frac{1}{2}$	16.84	5/2→ 3/2 , 7/2→ 3/2 , 5/2→ 5/2,7/2→ 5/2.
201	$\frac{3}{2}$	13.22	3/2 → 1/2 , 5/2 → 3/2 , 3/2 → 3/2 7/2 → 5/2 5/2 → 5/2 , 3/2 → 5/2 9/2 → 7/2 , 7/2 → 7/2 5/2 → 7/2.

The table presents data on the mass numbers, nuclear spins (I), abundances (as percentages), and transitions of the most common isotopes found in a small sample of mercury vapor.

Energy level diagram of ^{202}Hg

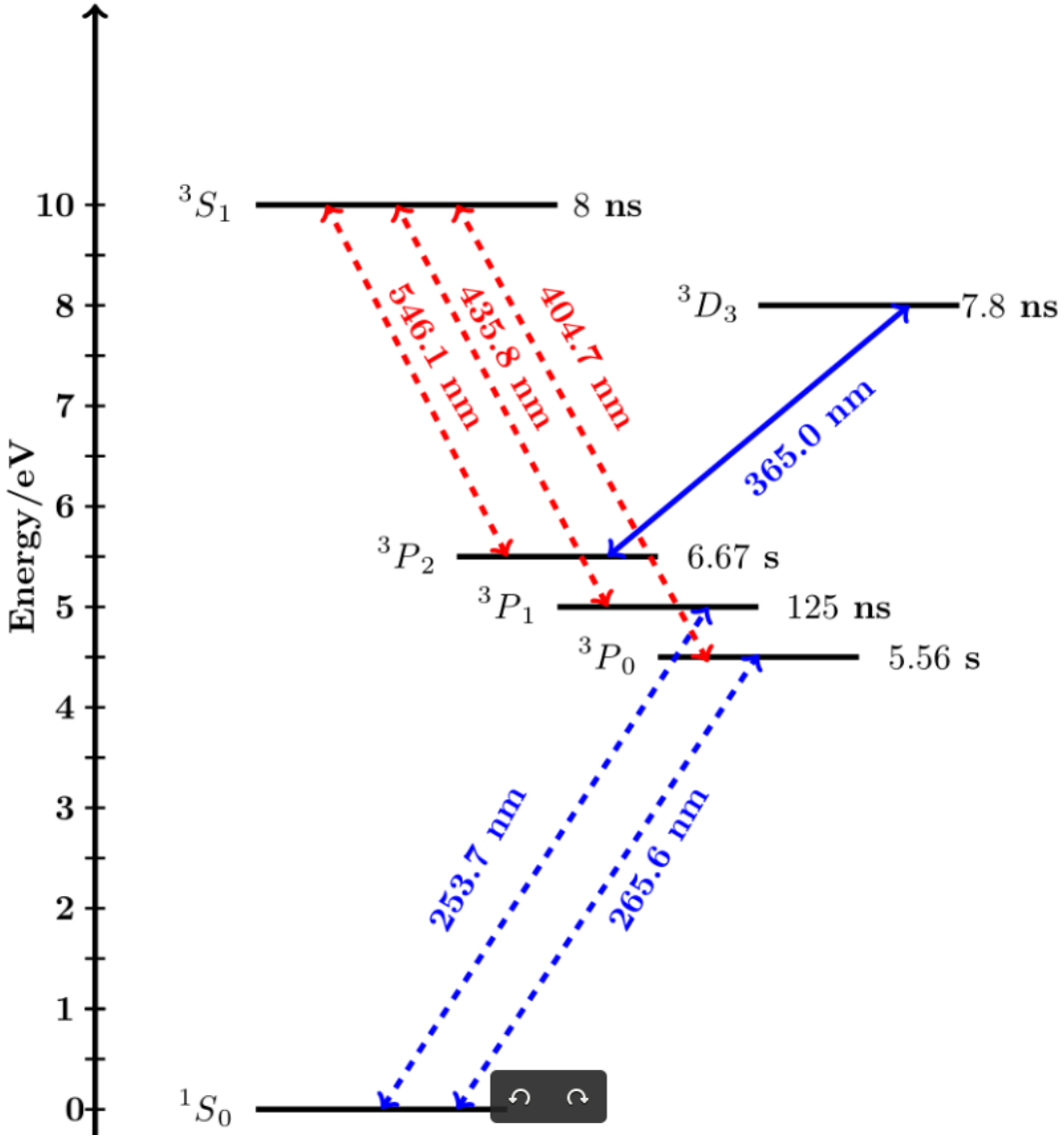

Homodyne detection $\hat{\mathrm{M}} = f_{lo}^{\dagger}\hat{\Omega}e^{-i\theta} + f_{lo}\hat{\Omega}^{\dagger}e^{i\theta}$

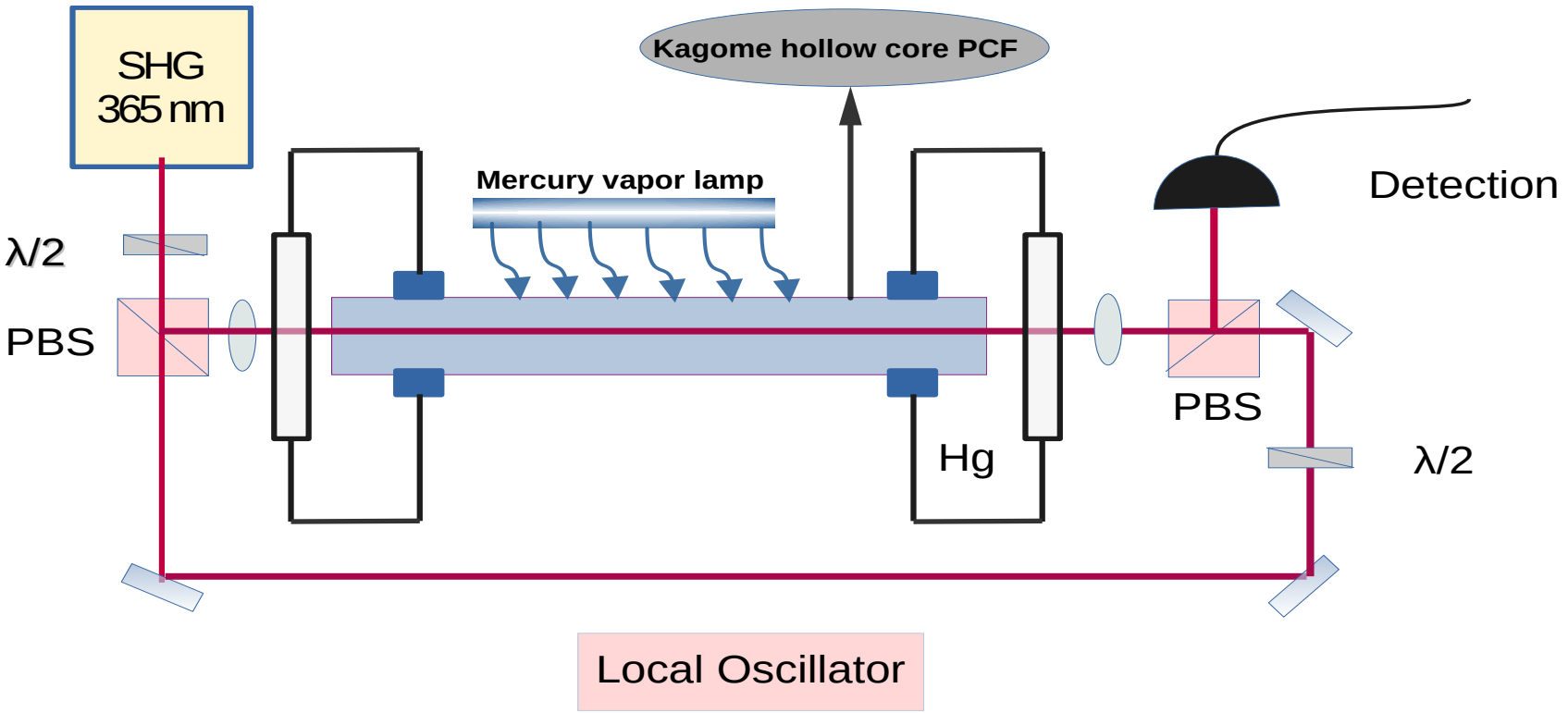

Isotope ^{202}Hg

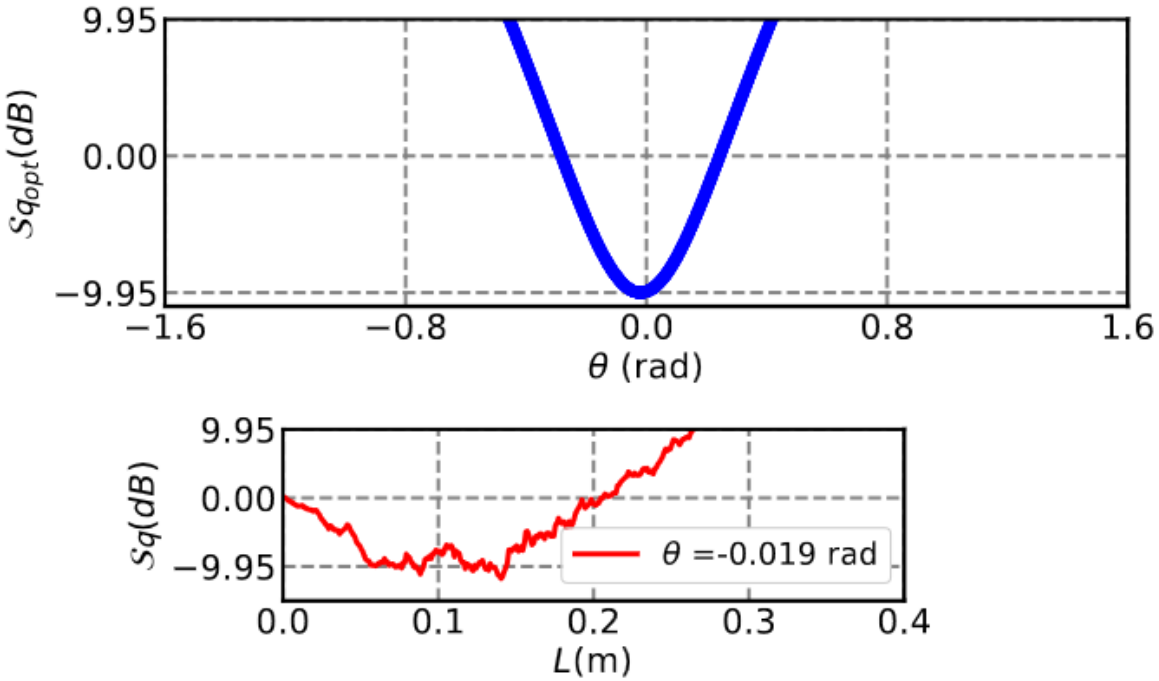

FIG. 3. The figure illustrates the quadrature squeezing characteristics for a pulse with an initial area of $\Theta_0 = 2\pi$ at resonance. In the upper subplot, the squeezing values are presented at $L = 0.1(\mathrm{m})$ for various detection angles. The lower subplot depicts the evolution of the optimum squeezing along the fiber length.

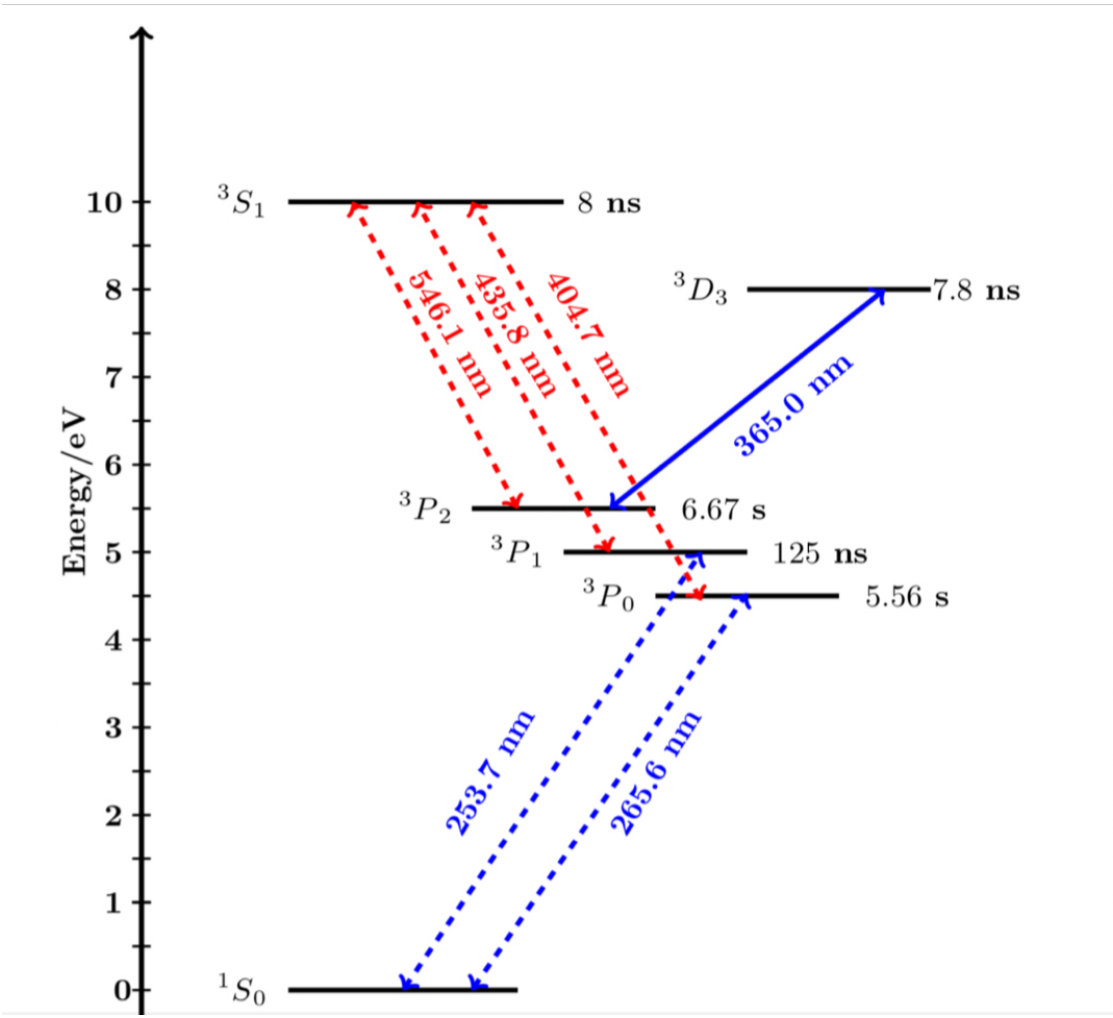
Energy/eV
10
8
7
6
5
4
3
2
1
0
$^3S_1$
8 ns
$^3D_3$
7.8 ns
$^3P_2$
6.67 s
$^3P_1$
125 ns
$^3P_0$
5.56 s
$^1S_0$
546.1 nm
435.8 nm
404.7 nm
365.0 nm
253.7 nm
265.6 nm

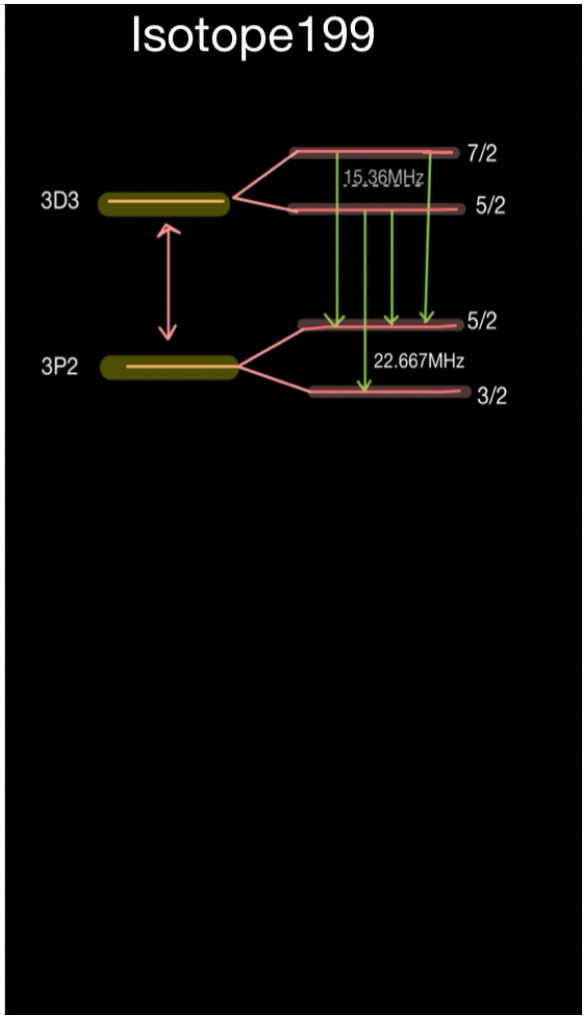
Isotope199
3D3
3P2
7/2
5/2
5/2
3/2
15.36MHz
22.667MHz

Caption

Squeezing in the room temperature